

Radial fractional-order dispersion through fractured rock

David A. Benson,¹ Charles Tadjeran,² Mark M. Meerschaert,³ Irene Farnham,⁴ and Greg Pohl¹

Received 29 April 2004; revised 14 October 2004; accepted 25 October 2004; published 28 December 2004.

[1] A solute transport equation with a fractional-order dispersion term is a model of solute movement in aquifers with very wide distributions of velocity. The equation is typically formulated in Cartesian coordinates with constant coefficients. In situations where wells may act as either sources or sinks in these models, a radial coordinate system provides a more natural framework for deriving the resulting differential equations and the associated initial and boundary conditions. We provide the fractional radial flow advection-dispersion equation with nonconstant coefficients and develop a stable numerical solution using finite differences. The hallmark of a spatially fractional-order dispersion term is the rapid transport of the leading edge of a plume compared to the classical Fickian model. The numerical solution of the fractional radial transport equation is able to reproduce the early breakthrough of bromide observed in a radial tracer test conducted in a fractured granite aquifer. The early breakthrough of bromide is underpredicted by the classical radial transport model. Another conservative, yet nonnaturally occurring solute (pentafluorobenzoate), also shows early breakthrough but does not conclusively support the bromide model due to poor detection at very low concentrations. The solution method includes, through a procedure called subordination, the effects of solute partitioning on immobile water. *INDEX TERMS*: 1832 Hydrology: Groundwater transport; 3230 Mathematical Geophysics: Numerical solutions; 3250 Mathematical Geophysics: Fractals and multifractals; 1869 Hydrology: Stochastic processes; *KEYWORDS*: fractional derivative, numerical method, radial dispersion, subordination

Citation: Benson, D. A., C. Tadjeran, M. M. Meerschaert, I. Farnham, and G. Pohl (2004), Radial fractional-order dispersion through fractured rock, *Water Resour. Res.*, 40, W12416, doi:10.1029/2004WR003314.

1. Introduction

[2] Owing to time constraints, tracer tests are often conducted under forced gradients. In particular, the radial flow regime induced by a pumping well is often used to estimate the parameters needed for prediction of long-term transport under natural gradients. The effective porosity (for velocity) and dispersivity (for the dispersion tensor) are two parameters that are used in a Fickian, second-order advection-dispersion governing equation of motion. The effect of the radial geometry, aquifer heterogeneity, and test size on the applicability and/or scale dependency of the estimates has been demonstrated by *Chao et al.* [2000] and *Reimus* [2003]. An alternative to a scale-dependent dispersion coefficient in a Fickian model is a fractional-order dispersion term, which accounts for a non-Fickian plume scaling rate and a heavy (power law) leading edge of the plume moving under natural gradient conditions [*Benson et al.*, 2001]. The fractional-order dispersion derivative is a consequence of a highly heterogeneous, power law distribution of

water velocities and long-range correlation or preferential flow [*Herrick et al.*, 2002; *Benson et al.*, 2000a; *Cushman and Ginn*, 2000]. In this study, a power law (fractal) distribution refers to the asymptotic relation $P(X > x) \sim x^{-b}$ for positive b [*Mandelbrot*, 1982]. A power law distribution, with $b < 2$, of solute particle travel distance over some period of time induces a fractional dispersion derivative, in tandem with linear drift (mean advection), in the governing equation of motion [*Saichev and Zaslavsky*, 1997; *Chaves*, 1998; *Benson*, 1998].

[3] While this study will focus on early arrivals to an extraction well, no analysis of breakthrough curves (BTC) can ignore the effects of solute retention and late-time tailing. Here we provide a brief review. Two primary models exist that represent end members of possible behavior. The mobile/immobile (MIM) model assumes that solute particles spend random amounts of time in an immobile phase. Solute that spends power law-distributed random amounts of time (with $b < 2$) in an immobile phase induces a fractional-order time derivative in the governing equation [*Schumer*, 2002; *Dentz and Berkowitz*, 2003; *Schumer et al.*, 2003; *Baeumer et al.*, 2005]. In the fractal MIM model, the two vastly different extreme behaviors that generate fractional space and time derivatives (rapid transport and long-term immobilization, respectively) are considered independent, or uncoupled [*Haggerty et al.*, 2000]. The uncoupling of immobilization time and the subsequent velocity allows simple computation of the breakthrough

¹Desert Research Institute, Reno, Nevada, USA.

²Department of Mathematics and Statistics, University of Nevada, Reno, Nevada, USA.

³Department of Physics, University of Nevada, Reno, Nevada, USA.

⁴Stoller Navarro Joint Venture, Las Vegas, Nevada, USA.

curves through a process called subordination [Feller, 1971; Schumer et al., 2003]. This process is also equivalent to uncoupled continuous time random walk (CTRW) models [Montroll and Weiss, 1965; Shlesinger et al., 1982; Grubert, 2001; Berkowitz et al., 2002; Dentz and Berkowitz, 2003; Bromly and Hinz, 2004; Cortis et al., 2004]. For solute transport, subordination replaces the deterministic clock time that a particle spends undergoing a motion process with a random “operational time.”

[4] On the other hand, Becker and Shapiro [2003] describe numerous BTC using a model in which tracer mass in any streamtube is fixed and proportional to the water flux in the streamtube. The retention is not due to random trapping in immobile zones. Instead, it is due to the presence of streamtubes with arbitrarily slow advection, so the retention is directly coupled to velocity. Certain types of coupled processes, along with the uncoupled process, generate unique fractional-order governing equations with some similar properties [Meerschaert et al., 2003]. For example, coupled and uncoupled models may have the same slope on a log-log plot of the BCT tail while the growth rates, hence peak arrival times, of the two plumes are completely different. Shlesinger et al. [1982] discuss the effect of coupling on growth rate. Furthermore, in the idealized fractal MIM model, all retention is within zero-velocity zones; therefore, solutes with different molecular diffusivity will have different retention and overall transport [Haggerty et al., 2000; Reimus et al., 2003]. In Becker and Shapiro’s [2003] model, all solutes experience the same nonzero velocity distribution and travel identically. It is highly likely that both the coupled and uncoupled mechanisms contribute to the overall retention in any single fractured system. The relative degree of either mechanism is best discerned using the extremely late breakthrough, since these solute particles have experienced either diffusive-limited transport or very slow coadvection. Different tests, using multiple tracers with significantly different diffusion coefficients, have been analyzed assuming one or the other model with good results [Becker and Shapiro, 2003; Haggerty et al., 2000; Reimus et al., 2003].

[5] To distinguish between the space and time operations, we call these effects fractional dispersion and fractal retention, respectively. In subsurface hydrology at the field scale, the fractional dispersion approach has only been used to model natural gradient tests in saturated, granular, aquifer material [Benson et al., 2000b, 2001]. A recent forced gradient test conducted in a fractured granite aquifer [Reimus et al., 2003] shows some of the characteristics of anomalous transport. The conservative bromide tracer arrives at the extraction well far in advance of the classical (Fickian) model. We theorize that flow in the fractures or fracture network is highly heterogeneous [see, e.g., Tsang and Tsang, 1987; Moreno et al., 1985, 1988, 1990; Haldeman et al., 1991; Thompson, 1991; Johns and Roberts, 1991; Brown, 1989; Mourzenko et al., 1995; Keller et al., 1999] and can be modeled with the fractional dispersion approach. Furthermore, the test shows the fingerprint of long-term solute retention, with incomplete mass recovery and anomalous late-time breakthrough. Reimus et al. [2003] use a classical advection-dispersion model of transport in the fractures, coupled to an immobile phase in identically sized matrix blocks, to fit the data. We formulate and solve the radial solute transport problem for a fractional-order disper-

sion derivative in order to better fit the early-time BTC, and include the effects of communication with an immobile phase with long-term waiting times in a manner similar to Haggerty et al. [2000], Reimus et al. [2003], Dentz and Berkowitz [2003], and Schumer et al. [2003]. An analysis of Becker and Shapiro’s [2003] coupled retention is beyond the scope of this study, and as we will show, not possible with the incomplete BTC tail data.

[6] If the time that a solute particle spends in a volume of immobile water (whether in-fracture or extra-fracture “matrix” water) is independent of the speed at which the particle travels when released back in the mobile fracture water, then the breakthrough curve can be solved using two independent models. The first is the transport in the mobile phase alone. This solution is then subordinated according to the distribution of random waiting times in an immobile phase [Schumer et al., 2003; Scalas et al., 2004]. We assume this independence (as do all MIM models) so that we can solve the spatially fractional problem in radial coordinates and simply transform the solution to include solute retention.

[7] Before deriving the fractional-order, radially convergent, mobile-phase transport equation, we begin with conservation of mass of a purely mobile solute in cylindrical coordinates [Hoopes and Harleman, 1967]:

$$\frac{\partial c}{\partial t} = -\frac{1}{r} \frac{\partial}{\partial r} [r q(r, t)] + f(r, t), \quad (1)$$

where $c = c(r, t)$ is the concentration of the solute (with radial symmetry), and $f(r, t)$ is a forcing function that may be used to model the injection or extraction of solute as a function of space and time. The total flux $q(r, t) = q_1(r, t) + q_2(r, t)$, where $q_1(r, t)$ is the common drift (mean advective) flux, and $q_2(r, t)$ is the dispersive flux (representing deviations from the common drift velocity). The classical Fickian model uses mean advective flux, defined by

$$q_1(r, t) = v(r)c,$$

and Fick’s Law for dispersive flux based on empirical observations, defined by

$$q_2(r, t) = -d(r) \frac{\partial c}{\partial r},$$

where $v(r)$ is the common drift velocity, and $d(r)$ is the dispersion coefficient, both of which are functions of the radius.

[8] In a uniform porous medium of thickness b with porosity θ , with a radial flow toward the extraction well pumping at rate Q , the advective velocity is given by

$$v(r) = \frac{Q}{2\pi b\theta r} = \frac{\kappa_v}{r}$$

for some constant $\kappa_v = Q/2\pi b\theta$. Moreover, a working assumption typically is made [Bear, 1972] or measured [e.g., Hoopes and Harleman, 1967] that the hydrodynamic dispersion coefficient at any point is proportional to the velocity. Therefore we may write

$$d(r) = \frac{a\kappa_v}{r}$$

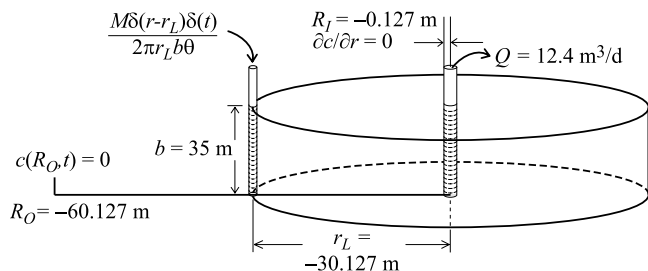


Figure 1. Schematic of tracer test and numerical boundary conditions.

for some constant dispersivity a . If these expressions for $v(r)$ and $d(r)$ are substituted in (1), then after some simple manipulations we obtain

$$\frac{\partial c}{\partial t} = -\frac{\kappa_v}{r} \frac{\partial c}{\partial r} + \frac{a\kappa_v}{r} \frac{\partial^2 c}{\partial r^2} + f(r, t), \quad (2)$$

subject to the appropriate initial and boundary conditions.

2. Radial Fractional Advection-Dispersion Equation

[9] Early arrivals of solute at an extraction well may not be predicted by the classical Fickian model. In natural gradient tests, a fractional-order Fick's Law is a model of anomalously rapid transport [Benson *et al.*, 2001; Paradisi *et al.*, 2001; Molz *et al.*, 2002]. In this case, the gradient of the solute concentration in the empirical flux equation is replaced by a nonlocal fractional derivative:

$$q_2(r, t) = -d(r) \frac{\partial^{\alpha-1} c(r, t)}{\partial r^{\alpha-1}},$$

where the fractional derivative on the right-hand side is defined by the domain of the problem (Appendix A). Since our radial flow problem exists within a finite domain, we use the Riemann-Liouville (with the corresponding Grünwald formulation) fractional derivative [Oldham and Spanier, 1974; Miller and Ross, 1993].

[10] The fractional term directly models anomalous dispersion due to extreme velocity contrasts. In the case of flow within fractures, the dominant mechanism is thought to be channeling of the flow into distinct preferential pathways [Moreno *et al.*, 1985; Tsang and Tsang, 1987; Brown, 1989]. Under this model, the velocity contrasts also lead to growth rate of a plume under natural gradient conditions faster than the Fickian rate of $t^{1/2}$ [Benson *et al.*, 2000b]. When this form of the dispersive flux is substituted into (1), we get

$$\frac{\partial c}{\partial t} = -\frac{\kappa_v}{r} \frac{\partial c}{\partial r} + \frac{a\kappa_v}{r} \frac{\partial^\alpha c}{\partial r^\alpha} + f(r, t). \quad (3)$$

The forcing function can model the injection of the solute at the injection well. The units of a are $L^{\alpha-1}$ so that $d(r) = a\kappa_v/r$ has dimension L^α/T . A mass conservative and nonnegative solution requires that $0 < \alpha \leq 2$. For convenience we assume $v(r) \geq 0$ and $d(r) \geq 0$ so that the flow is from left to right in the finite domain between left

and right (outer and inner) boundaries $R_O < r < R_I$. This induces a somewhat unorthodox coordinate system with $r \leq 0$ that works naturally with the directional fractional derivative (Appendix A). In general we may assume an initial condition $c(r, t = 0) = F(r)$ for $R_O < r < R_I$ and a natural set of boundary conditions for this problem: $c(r = R_O, t) = 0$ for all $t \geq 0$ and $\partial c(r = R_I, t)/\partial r = 0$ for all $t \geq 0$ (Figure 1). Physically, the boundary conditions mean that no tracer leaks past the outer boundary, and that the tracer moves by advection through the inner boundary (and into the extraction well). No solute may diffuse or disperse out of the extraction well into the formation. Since our problem models the effluent from an extraction well, $c(r, t)$ represents the flux-averaged concentration; however, since $\partial c(r = R_I, t)/\partial r = 0$, the resident and flux concentrations are equivalent at the extraction well [Moench, 1989].

[11] The fractional derivative formulation is a generalization of the standard model, and provides a fractional-order parameter that can be estimated to properly model the arrival of the solute at the extraction well. See Benson *et al.* [2001] and Herrick *et al.* [2002] for some practical methods of estimating the order α of the fractional derivative from hydraulic conductivity data. Analytic solutions to the fractional PDE (3) are elusive, but do exist for some analytic expressions of v , d , and f . In general, the resulting spatially fractional advection dispersion equation is solved by numerical methods and can be validated against the few analytic solutions [Meerschaert and Tadjeran, 2003].

[12] An implicit Euler method, based on a modified Grünwald approximation to the fractional derivative, (or a similarly defined Crank-Nicholson finite difference method) is a consistent and unconditionally stable numerical solution [Meerschaert and Tadjeran, 2003]. We use this method to provide convergent numerical solutions for the fractional radial flow equation with variable velocity and dispersion coefficients (Appendix A).

3. Temporal Subordination

[13] If the mobile solute equation is an appropriately defined Cauchy problem $\partial c/\partial t = Ac + F(r)\delta(t)$, where $A(r)$ is a time-homogeneous advection-dispersion operator (for example, a boundary value problem with equation (3)), and $F(r) = c(r, t = 0)$ is the initial condition, then the addition of infinite mean, heavy-tailed random waiting times in an immobile phase induces an equation for the mobile phase of [Schumer *et al.*, 2003; Dentz and Berkowitz, 2003]

$$\frac{\partial c}{\partial t} + \beta \frac{\partial^\gamma c}{\partial t^\gamma} = Ac - \frac{F(r)\beta t^{-\gamma}}{\Gamma(1-\gamma)}, \quad (4)$$

where $\beta[T^{\gamma-1}]$ is a fractal capacity coefficient, $0 < \gamma \leq 1$, and the Caputo fractional time derivative is defined by its Laplace transform $s^{\gamma-1}(s\hat{c}(r, s) - c(r, t = 0))$. The solution may be gained by first solving the mobile-only solution $\partial m/\partial t = Am + F(r)\delta(t)$ and subordinating the result via the integration

$$c(r, t) = \int_0^t m(r, u) g_\gamma \left(\frac{t-u}{(\beta u)^{1/\gamma}} \right) (\beta u)^{-1/\gamma} du,$$

where the function $g_\gamma(t)$ with Laplace transform $\hat{g}(s) = \exp(-s^\gamma)$ is the probability density function of the limit of

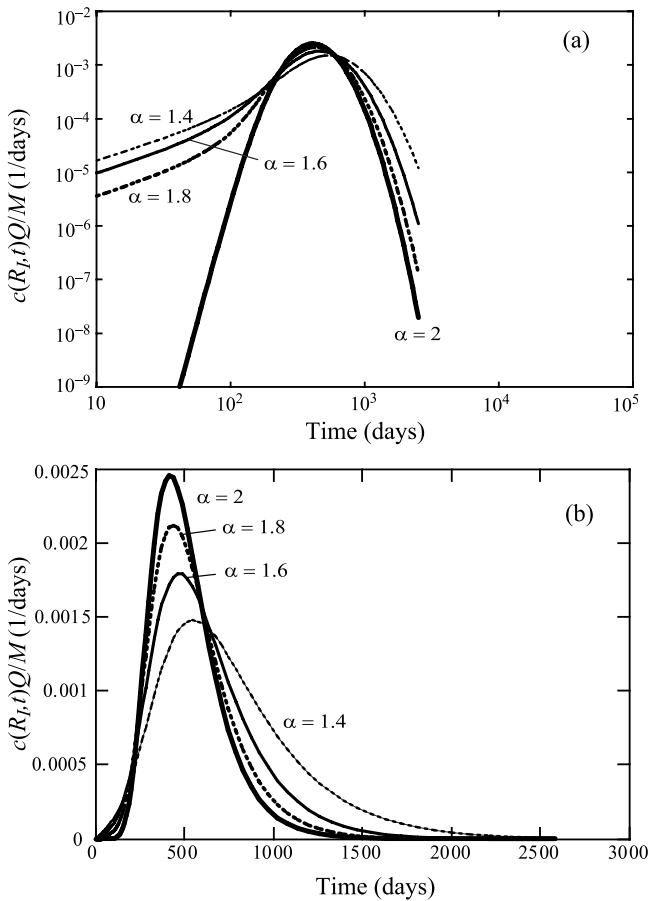


Figure 2. Log-log and linear plots of normalized concentration ($c(R_f, t)Q/M$) at a central well for several values of the fractional dispersion parameter α . Solute undergoing Fickian dispersion and no partitioning to an immobile phase is shown by the curve $\alpha = 2$. See color version of this figure in the HTML.

an appropriately scaled sum of heavy-tailed waiting times [Schumer et al., 2003]. A subordination integral [Feller, 1971] accounts for the fact that a particle participates in the equation of motion (1) for only a portion of the “clock” time. The long-time tail of $g_\gamma(t)$ decays like $t^{-1-\gamma}$, so this formulation includes the diffusion of solutes into infinite matrix blocks with a return time density with $\gamma = 1/2$ [e.g., Tsang, 1995; Haggerty et al., 2000]. Long-term tests in fractured [Haggerty et al., 2000] and granular [Schumer et al., 2003] aquifers indicate different values of γ between zero and unity.

4. Model Properties

[14] The novel elements of the model (4), when a radial fractional dispersion model is used for the purely mobile phase, are the orders of the dispersion derivative (α) and the time derivative (γ). Using the same boundary value problem defined by the Shoal tracer test (Figure 1, described in section 5) and holding all other parameters constant ($\kappa_v = a = 1$), we investigate the effect of varying both of these derivatives. When $\gamma = 1$, the term $(1 + \beta)$ is identical to the classical retardation coefficient, so we first set $\beta = 0$

and vary α over the set [2.0, 1.8, 1.6, 1.4]. The most notable effect of decreased α is the early arrival of the leading edge of the plume (Figure 2). This is accompanied by an overall increase in the width of the breakthrough curve.

[15] To illustrate the effect of the fractional time derivative, we hold $\alpha = 2$ and $\beta = 0.005$ and vary γ over the set [0.3, 0.4, 0.5, 0.6, 0.7, 1.0]. When $0 < \gamma < 1$ the late-time breakthrough curve (Figure 3a) decays like $c(r, t) \sim t^{-1-\gamma}$ [Haggerty et al., 2000; Schumer et al., 2003; Dentz and Berkowitz, 2003]. Lower values of γ , with the same capacity coefficient β , have a clearly reduced peak concentration and somewhat delayed peak arrival time, both due to the increased proportion of long times in an immobile phase (Figure 3b). The effects of the fractional space and time derivatives are, for the most part, independent. Each non-integer order derivative adds a “wing” to the Fickian BTC.

5. Application

[16] In a recent field study conducted in a fractured granite aquifer [Reimus et al., 2003], a predominantly radial flow regime was induced by pumping an extraction well at a rate of $Q = 16.3 \text{ m}^3/\text{day}$ and reinjecting approximately 10% of the water into the eventual tracer injection well. Upon

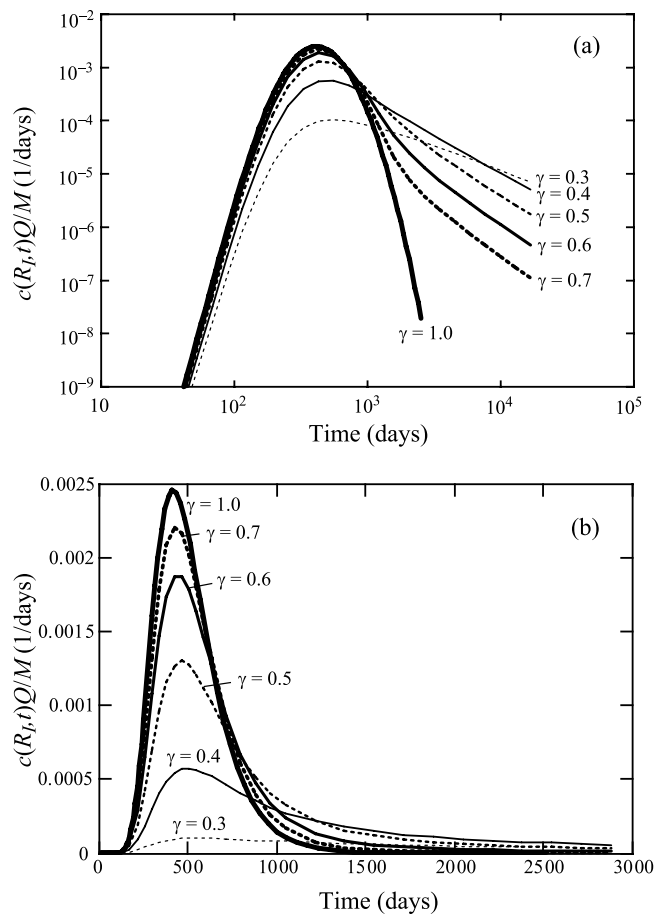


Figure 3. Log-log and linear plots of normalized concentration ($c(R_f, t)Q/M$) at a central well for several values of the immobile parameter γ . Purely mobile solute undergoing Fickian dispersion is shown by the curve $\gamma = 1.0$. See color version of this figure in the HTML.

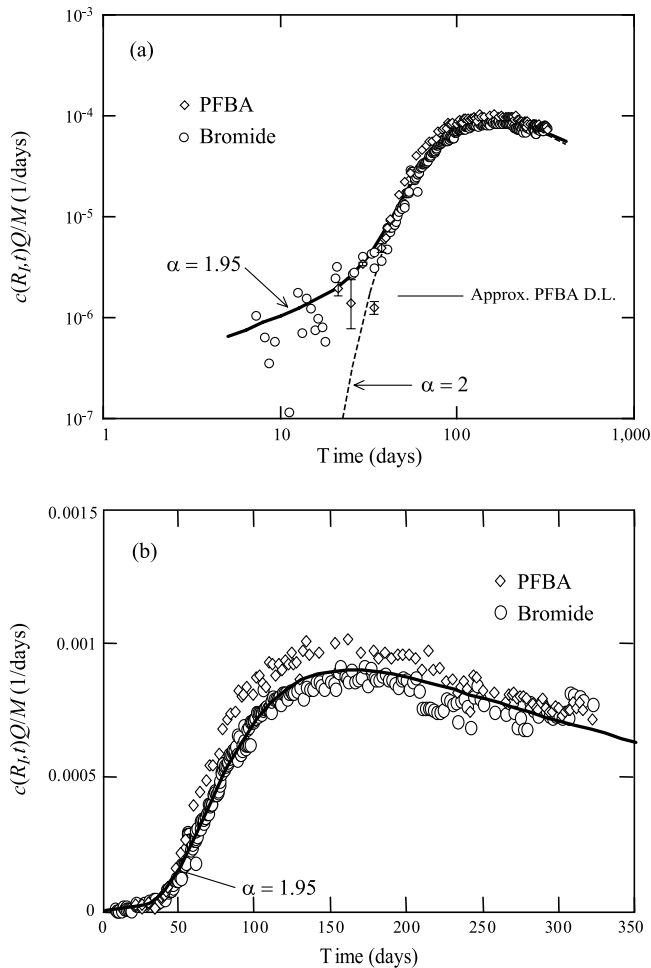


Figure 4. Log-log and linear plots of normalized bromide and PFBA concentration at the extraction well. A fractional radial flow model with $\alpha = 1.95$ captures the early breakthrough. Early PFBA data are shown plus/minus one standard deviation. See color version of this figure in the HTML.

reaching a relatively steady state, a mixture of two conservative solutes and one sorbing solute were introduced at the injection well for a period of 3.54 days. Within the mixture, 20.81 kg of bromide, at an average concentration of 3.77 kg/m^3 , and 2.19 kg of pentafluorobenzoate (PFBA) at an average concentration of 0.397 kg/m^3 were included. Samples from the extraction well were separately analyzed for both of these relatively conservative solutes using ion chromatography for bromide and high-pressure liquid chromatography for PFBA. Over the course of the test, the extraction rate declined steadily, giving an average extraction rate of approximately $Q = 12.4 \text{ m}^3/\text{day}$. The distance from the injection well to the extraction well is 30 m, and the radius of the extraction well is 0.127 m. The extraction well screened interval is 35 m, so $v(r) = Q/2\pi r b \theta = 0.0564/(r\theta) \text{ m}^2/\text{day}$, and $d(r) = av(r)$. This gives two parameters that describe the velocity and dispersion: the mobile, or effective, porosity θ and the dispersivity a . The remaining fitting parameters are the fractional dispersion order α , describing anomalously early arrivals, and the order and capacity coefficient of the heavy-tailed waiting times γ and β . For

diffusion from a single smooth fracture of constant aperture b into infinite immobile slabs, $\gamma = 1/2$ and $\beta = \phi\sqrt{D_m}/b$, where ϕ is the matrix porosity, and D_m is the diffusion coefficient in the matrix [Haggerty et al., 2000; Reimus et al., 2003].

[17] In the numerical solution (Figure 1), we use outer and inner boundaries to the radial domain of $R_O = -60.127 \text{ m}$ and $R_I = -0.127 \text{ m}$. The injection well is at $r_L = -30.127 \text{ m}$, the extraction well is centered at $r = 0$, with its wall at $r = R_I = -0.127 \text{ m}$. Both are assumed to have negligible well bore mixing. The outer boundary is set to be upstream and sufficiently far from the injection well so that no measurable bromide concentration reaches the outer boundary during the time of interest. Therefore we may assume $c(r = R_O, t) = 0$, and $\partial c(r = R_I, t)/\partial r = 0$. The injection of solutes occurred over a short enough time period, followed by flushing, that the forcing function is approximated by a Dirac delta function in space and time $f(r, t) = M\delta(r - r_L)\delta(t)/2\pi r_L b \theta$, where M is the injected mass (Figure 1).

[18] A graph of bromide concentration at the extraction well as a function of time, along with the results of numerical estimates using the subordinated implicit Euler method are shown in Figure 4. All concentrations are normalized by the factor Q/M so that complete recovery of the solute would integrate to unity. We find that the hydraulic parameters $\theta = 0.015$, $a = 2 \text{ m}^{0.95}$, $\alpha = 1.95$ and temporal subordination parameters $\gamma = 1/2$ and $\beta = 0.116 \text{ day}^{-1/2}$ provide a fit to most of the data. In agreement with Reimus et al.'s [2003] analysis of the data, we find that the problem is highly nonunique: since the dispersivity and retention within an immobile matrix both serve to spread the solute arrival, a large set of parameters fit the data equally well. Unfortunately, the test was stopped before sufficient data could uniquely resolve the late-time tail parameters γ and β (compare Figures 3a and 4a). However, we wish to stress that a space-fractional derivative of order $\alpha < 2$ seems necessary to capture the early-time arrivals, and a time-fractional derivative of order $\gamma < 1$ was required to fit the late arrivals. The classical radial flow model (Figure 4a) greatly underestimates the early arrival of bromide. For reference, the parameters in the classical $\alpha = 2$ model shown in Figure 4 are $\theta = 0.026$, $a = 5 \text{ m}$, $\gamma = 1/2$, and $\beta = 0.065 \text{ day}^{-1/2}$, although a range of parameters fit equally well.

[19] The lack of complete tail data also does not allow us to differentiate between tailing models based on diffusion into immobile water versus slow advection. For these reasons we choose $\gamma = 1/2$, which is the standard solution for diffusion into infinite immobile slabs. The $\gamma = 1/2$ solution is the genesis for the “ $-3/2$ law” describing the slope of the late-time BTC on a log-log plot [see, e.g., Tsang, 1995; Haggerty et al., 2000]. The fractional radial flow model captures the early breakthrough of bromide at the extraction well, as well as the late-time tailing. The (normalized) PFBA breakthrough is very similar to the that of bromide, suggesting either that the slow pathways are not primarily due to diffusion into stagnant zones [e.g., Becker and Shapiro, 2003] or that a significant portion of the injected mass is not within the capture zone of the extraction well [Reimus et al., 2003].

[20] PFBA samples collected prior to 37 days were reported as containing less than the detection limit. To

investigate whether early breakthrough of bromide is indeed anomalous, we inspected the chromatograms provided by the Harry Reid Center (Las Vegas, NV) for the PFBA analysis. The chromatograms for early samples collected from 20 to 37 days show peaks at retention times similar to PFBA, though the peaks are not always statistically significantly greater than background noise. We used the PFBA peak areas listed on the chromatograms and show the mean over multiple sample injections plus or minus one standard deviation (Figure 4a). While the PFBA data show wide scatter and hover close to the statistically significant detection limit, they do tend to show anomalously early arrival relative to the Fickian model (Figure 4a). However, due to the poor reliability of the PFBA data, we do not consider this a confirmation or a repudiation of the fractional transport model at this site. An artificial tracer with extremely low detection limits (e.g., DNA strands [Sabir *et al.*, 1999]) could be useful in the accurate determination of fast pathways modelled by a fractional dispersion term.

[21] The fractal MIM model with $\gamma = 1/2$ reproduces the recovery of roughly 20% of the bromide mass by the end of the test, and predicts that only about 80% of the mass would be recovered if the test were run forever, due to the irreversible loss of mass to an immobile phase. Furthermore, our values of $\beta = \phi\sqrt{D_m}/b = 0.065 \text{ d}^{-1/2}$ and $0.116 \text{ d}^{-1/2}$ for the classical and fractional dispersion models are approximately two to four times larger than reported by Reimus *et al.* [2003]. Our values are larger because we assume that all of the injected mass is within the extraction well capture zone. Since $\phi = 0.01$ to 0.02 and $D_m = 1.0 \times 10^{-6}$ to $1.7 \times 10^{-6} \text{ m}^2/\text{day}$ are measured and fixed values, our estimate of the fracture aperture is approximately two to four times smaller than Reimus *et al.*'s [2003] reported range of 0.6 to 13 mm.

6. Discussion

[22] This paper develops a fractional radial flow equation, and applies the equation to model breakthrough curves from a forced-gradient tracer test in fractured granite [Reimus *et al.*, 2003]. The model uses a fractional partial differential equation with spatially variable coefficients. Numerical solutions are obtained using a novel implicit Euler method to handle the fractional space derivative, and a standard subordination to take care of the fractional time derivative. The space-fractional derivative models anomalous superdispersion, which causes tracer to arrive earlier than the classical Fickian model predicts. Bromide arrival at the pumping well is modeled by a spatially fractional derivative of order $\alpha = 1.95$, indicating weak superdispersion that can be attributed to mild heterogeneity of velocities in the fracture(s) [Schumer *et al.*, 2001]. While close to the classical $\alpha = 2$ space derivative, this fractional derivative term is still important for capturing the very early arrivals (Figure 4a). A model of the entire BTC required a model of retention, which we chose to be diffusion into large (effectively infinite) matrix blocks. This type of retention can be modeled by a fractional time derivative of order $\gamma = 1/2$, and would not only retard, but counteract the superdiffusive growth rate of a plume travelling under natural gradient conditions [Schumer *et al.*, 2003; Dentz and Berkowitz, 2003].

[23] Bromide is a naturally occurring element that imparts noise and poor detection limits to early, low-concentration data. In an attempt to verify that anomalous superdispersion is really taking place, we also examined the breakthrough curve for another nonreactive tracer. This nonnaturally occurring tracer (PFBA) also shows evidence of non-Fickian early arrivals, but poor detection at low concentrations makes this evidence inconclusive. In the study of toxic solutes, it is most important to have reliable models of the leading edge of the breakthrough curve. The scatter in the bromide and PFBA data suggests that better tracers are needed: ones that are not found in nature, do not interact significantly with the aquifer solids, and are detectable at extremely low concentrations. For example, the detection of minute amounts of designer DNA tracer in the Moreppen test [Sabir *et al.*, 1999] show that the extreme edges of a plume grow much faster than those outlined by mg/l or $\mu\text{g/l}$ levels of traditional tracers like bromide, and indicates that new tracers are needed to test new models.

[24] Analyses of tests in fractured rock by Becker and Shapiro [2003] and McKenna *et al.* [2001] do not indicate the anomalously early breakthrough of extremely low concentrations. Thus the early arrivals may not be a ubiquitous occurrence in fractured rock, or simply may be difficult to detect using standard techniques. The data in the present case show only weak heterogeneity, suggesting that short-range transport in fractured rock may be nearer to Fickian behavior than in strongly heterogeneous granular material. On the other hand, a heavy late-time tail on a breakthrough curve is very commonly observed in tracer tests, so the applicability of the more general mobile/immobile, CTRW, or time-fractional models (4) is well established. Fractally distributed travel velocities and/or retention times imply using a flow equation that accommodates fractional derivatives in both space and time, in order to allow for the possibility of superdispersion (modeled by a fractional space derivative) as well as retardation, subdiffusion, and loss of mobile mass (modeled by a fractional time derivative).

Appendix A: Numerical Methods

[25] We discuss the basic theory for numerical solution of the fractional advection-dispersion equation (3) on a finite domain $R_O < r < R_I$ with the initial condition $c(r, t = 0) = F(r)$ for $R_O \leq r \leq R_I$, and the boundary conditions $c(r = R_O, t) = 0$ and $\partial c(r = R_I, t)/\partial r = 0$ for all $t \geq 0$. Numerical methods for the spatially fractional advection-dispersion equation contain some surprises. The implicit (Euler) methods are the preferred approach to discretize the classical PDEs due to their unconditional stability which does not constrain the size of the time step. However, for the fractional ADE with the standard Grünwald estimates, the implicit Euler method (or the Crank-Nicholson method) is unconditionally unstable, while the explicit Euler method can be stable, albeit under a severe stepsize restriction. The situation can be remedied by the use of a shifted Grünwald formula which allows the implicit Euler method (and also the Crank-Nicholson method) to be unconditionally stable. For the shifted Grünwald formula the function evaluations are shifted to the right. The shifted Grünwald formula produces an unconditionally stable

finite difference method which is $O(h)$ consistent. For proof of these remarks refer to *Meerschaert and Tadjeran* [2003].

[26] A Riemann-Liouville fractional derivative on the finite interval $R_O \leq r \leq R_I$ may be defined (in the sense of generalized functions such as $\delta(r)$) as a convolution with a power law [*Oldham and Spanier*, 1974; *Samko et al.*, 1993]:

$$\frac{\partial^\alpha c(r, t)}{\partial r^\alpha} = \frac{1}{\Gamma(-\alpha)} \int_0^{r-R_O} y^{-1-\alpha} c(r-y, t) dy.$$

This is equivalent to Grünwald's infinite sum

$$\frac{\partial^\alpha c(r, t)}{\partial r^\alpha} = \frac{1}{\Gamma(-\alpha)} \lim_{M \rightarrow \infty} \frac{1}{h^\alpha} \sum_{k=0}^M \frac{\Gamma(k-\alpha)}{\Gamma(k+1)} c(r-kh, t), \quad (A1)$$

where $\Gamma(\cdot)$ is the gamma function. This leads to an approximation of the Riemann-Liouville fractional derivative by using a finite number (M) of terms, so that $h = (R_O - r)/M$ [*Miller and Ross*, 1993; *Podlubny*, 1999; *Samko et al.*, 1993]. Note that the value of the fractional derivative at a point r depends on the function values at that point and all the points at larger radii out to the outer boundary R_O . If we define the "normalized" Grünwald weights by

$$g_k = \frac{\Gamma(k-\alpha)}{\Gamma(-\alpha) \Gamma(k+1)}. \quad (A2)$$

Then the above Grünwald formula may be written

$$\frac{\partial^\alpha c(r, t)}{\partial r^\alpha} \approx \frac{1}{h^\alpha} \sum_{k=0}^M g_k c(r-kh, t). \quad (A3)$$

[27] Also note that these normalized weights only depend on the order α and the index k . The first four terms of this sequence are given by $g_0 = 1$, $g_1 = -\alpha$, $g_2 = \alpha(\alpha - 1)/2!$, $g_3 = -\alpha(\alpha - 1)(\alpha - 2)/3!$.

[28] Given a numerical approximation scheme, we define $t_n = n\Delta t$ to be the integration time $0 \leq t_n \leq T$, $\Delta r = h > 0$ is the grid size in space, $K = (R_I - R_O)/h$, $r_i = R_O + ih$ for $i = 0, \dots, K$ so that $R_O \leq r_i \leq R_I$, and c_i^n is the numerical approximation to $c(r_i, t_n)$. Similarly $d_i = d(r_i)$, $v_i = v(r_i)$, $f_i^n = f(r_i, t_n)$.

[29] It can be shown that the implicit Euler (or Crank-Nicholson) approach using the standard Grünwald formula results in an unconditionally unstable method [*Meerschaert and Tadjeran*, 2003]. To obtain a stable (and a convergent) finite difference method, we define and use a shifted Grünwald formulation. The shifted Grünwald formula takes the following form:

$$\frac{\partial^\alpha c(r, t)}{\partial r^\alpha} = \lim_{M \rightarrow \infty} \frac{1}{h^\alpha} \sum_{k=0}^M g_k c[r - (k-1)h, t], \quad (A4)$$

from which an approximating formula for the fractional term can be defined by

$$\frac{\partial^\alpha c(r_i, t_n)}{\partial r^\alpha} \approx \frac{1}{h^\alpha} \sum_{k=0}^i g_k c_{i-k+1}^n. \quad (A5)$$

Note that for $\alpha = 2$, which corresponds to the classical second derivative case, (A5) is just the standard centered difference formula for approximating the second derivative ($g_0 = 1$, $g_1 = -2$, $g_2 = 1$, $g_3 = g_4 = \dots = 0$),

$$\frac{\partial^2 c(r_i, t_n)}{\partial r^2} \approx \frac{c_{i+1}^n - 2c_i^n + c_{i-1}^n}{h^2}. \quad (A6)$$

[30] When the shifted Grünwald estimate (A5) is substituted in the implicit Euler method, the resulting difference equations are

$$\frac{c_i^{n+1} - c_i^n}{\Delta t} = -v_i \frac{c_i^{n+1} - c_{i-1}^{n+1}}{h} + \frac{d_i}{h^\alpha} \sum_{k=0}^i g_k c_{i-k+1}^{n+1} + f_i^{n+1}. \quad (A7)$$

These equations, together with the boundary conditions ($c_0^{n+1} = 0$, $c_M^{n+1} = c_{M-1}^{n+1}$), result in a linear system of equations whose coefficient matrix is the sum of a lower triangular and a superdiagonal matrices. Defining $E_i = v_i \Delta t / h$, and $B_i = d_i \Delta t / h^\alpha$, then the system defined by (A7) can be rewritten:

$$c_i^{n+1} - c_i^n = -E_i (c_i^{n+1} - c_{i-1}^{n+1}) + B_i \sum_{k=0}^i g_k c_{i-k+1}^{n+1} + \Delta t f_i^{n+1}.$$

The above equation can be rearranged for the like terms to yield

$$\begin{aligned} & -g_0 B_i c_{i+1}^{n+1} + (1 + E_i - g_1 B_i) c_i^{n+1} - (E_i + g_2 B_i) c_{i-1}^{n+1} \\ & - B_i \sum_{k=3}^i g_k c_{i-k+1}^{n+1} = c_i^n + \Delta t f_i^{n+1}. \end{aligned}$$

[31] This difference equation defines a linear system of equations $\underline{A} \underline{C}^{n+1} = \underline{C}^n + \Delta t \underline{F}^{n+1}$ where

$$\begin{aligned} \underline{C}^{n+1} &= [c_0^{n+1}, c_1^{n+1}, c_2^{n+1}, \dots, c_K^{n+1}]^T, \\ \underline{C}^n + \Delta t \underline{F}^n &= [0, c_1^n + \Delta t f_1^n, c_2^n + \Delta t f_2^n, \dots, c_{K-1}^n + \Delta t f_{K-1}^n, 0]^T, \end{aligned}$$

and $\underline{A} = [A_{i,j}]$ is the matrix of coefficients. These coefficients, for $i = 1, \dots, K - 1$ and $j = 1, \dots, K - 1$ are defined as follows (note that $g_0 = 1$, $g_1 = -\alpha$):

$$A_{i,j} = \begin{cases} 0, & \text{when } j \geq i + 2 \\ -g_0 B_i, & \text{when } j = i + 1 \\ 1 + E_i - g_1 B_i, & \text{when } j = i \\ -E_i - g_2 B_i, & \text{when } j = i - 1 \\ -g_{i-j+1} B_i, & \text{when } j \leq i - 1, \end{cases}$$

while $A_{0,0} = 1$, $A_{0,j} = 0$ for $j = 1, \dots, K$, $A_{K,K} = 1$, $A_{K,K-1} = -1$, and $A_{K,j} = 0$ for $j = 0, \dots, K - 2$. The system of equations $\underline{A} \underline{C}^{n+1} = \underline{C}^n + \Delta t \underline{F}^{n+1}$ is solved at time t_n to advance the solution to time t_{n+1} .

[32] Note that in the present case, the coefficients are independent of time t , so the linear system needs to be solved only once, and the matrix multipliers saved to efficiently solve the resulting system of equations as the solution is marched forward in time. A similar approach applies to a more general boundary condition of the third kind of the form $c(R_f, t) + \eta \partial c(R_f, t) / \partial r = s(t)$.

[33] The Crank-Nicholson discretization, using the shifted Grünwald estimates for the fractional derivative, can also be shown to be unconditionally stable. The general preference for the Crank-Nicholson for the classical PDEs is that it provides a stable finite difference method that is second-order accurate $O((\Delta t)^2) + O(h^2)$. However, the Grünwald estimates (standard or shifted) are only $O(h)$ accurate, and therefore in the fractional advection-dispersion differential equations the second-order accuracy in time and space is not achieved by the use of the corresponding finite differences.

[34] **Acknowledgments.** This work was supported by NSF grants DMS-0139927, DMS-0139943, DMS-0417972, EAR-9980484, EAR-9980489, and US DOE grant DE-FG03-98ER14885. We thank anonymous reviewers and the Associate Editor for excellent comments.

References

- Baeumer, B., D. A. Benson, and M. M. Meerschaert (2005), Advection and dispersion in time and space, *Physica A*, in press.
- Bear, J. (1972), *Dynamics of Fluids in Porous Media*, Dover, Mineola, N. Y.
- Becker, M. W., and A. M. Shapiro (2003), Interpreting tracer breakthrough tailing from different forced-gradient tracer experiment configurations in fractured bedrock, *Water Resour. Res.*, *39*(1), 1024, doi:10.1029/2001WR001190.
- Benson, D. A. (1998), *The Fractional Advection-Dispersion Equation: Development and Application*, Ph.D. thesis, Univ. of Nev., Reno.
- Benson, D. A., S. W. Wheatcraft, and M. M. Meerschaert (2000a), Application of a fractional advection-dispersion equation, *Water Resour. Res.*, *36*, 1403–1412.
- Benson, D. A., S. W. Wheatcraft, and M. M. Meerschaert (2000b), The fractional-order governing equation of Lévy motion, *Water Resour. Res.*, *36*, 1413–1424.
- Benson, D. A., R. Schumer, M. M. Meerschaert, and S. W. Wheatcraft (2001), Fractional dispersion, Lévy motion, and the MADE tracer tests, *Transp. Porous Media*, *42*, 211–240.
- Berkowitz, B., J. Klafter, R. Metzler, and H. Scher (2002), Physical pictures of transport in heterogeneous media: Advection-dispersion, random-walk, and fractional derivative formulations, *Water Resour. Res.*, *38*(10), 1191, doi:10.1029/2001WR001030.
- Bromly, M., and C. Hinz (2004), Non-Fickian transport in homogeneous unsaturated repacked sand, *Water Resour. Res.*, *40*, W07402, doi:10.1029/2003WR002579.
- Brown, S. R. (1989), Transport of fluid and electric current through a single fracture, *J. Geophys. Res.*, *94*, 9429–9438.
- Chao, H.-C., H. Rajaram, and T. Illangasekare (2000), Intermediate-scale experiments and numerical simulations of transport under radial flow in a two-dimensional heterogeneous porous medium, *Water Resour. Res.*, *36*, 2869–2884.
- Chaves, A. (1998), Fractional diffusion equation to describe Lévy flights, *Phys. Rev. A*, *239*, 13–16.
- Cortis, A., C. Gallo, H. Scher, and B. Berkowitz (2004), Numerical simulation of non-Fickian transport in geological formations with multiple-scale heterogeneities, *Water Resour. Res.*, *40*, W04209, doi:10.1029/2003WR002750.
- Cushman, J. H., and T. R. Ginn (2000), Fractional advection-dispersion equation: A classical mass balance with convolution-Fickian flux, *Water Resour. Res.*, *36*, 3763–3766.
- Dentz, M., and B. Berkowitz (2003), Transport behavior of a passive solute in continuous time random walks and multirate mass transfer, *Water Resour. Res.*, *39*(5), 1111, doi:10.1029/2001WR001163.
- Feller, W. (1971), *An Introduction to Probability Theory and Its Applications*, vol. 2, 2nd ed., John Wiley, Hoboken, N. J.
- Grubert, D. (2001), Effective dispersivities for a two-dimensional periodic fracture network by a continuous time random walk analysis of single-intersection simulations, *Water Resour. Res.*, *37*, 41–50.
- Haggerty, R., S. E. McKenna, and L. C. Meigs (2000), On the late-time behavior of tracer test breakthrough curves, *Water Resour. Res.*, *36*, 3467–3479.
- Haldeman, W. R., Y. Chuang, T. C. Rasmussen, and D. D. Evans (1991), Laboratory analysis of fluid flow and solute transport through a fracture embedded in porous tuff, *Water Resour. Res.*, *27*, 53–65.
- Herrick, M. G., D. A. Benson, M. M. Meerschaert, and K. R. McCall (2002), Hydraulic conductivity, velocity, and the order of the fractional dispersion derivative in a highly heterogeneous system, *Water Resour. Res.*, *38*(11), 1227, doi:10.1029/2001WR000914.
- Hoopes, J. A., and D. R. F. Harleman (1967), Dispersion in radial flow from a recharging well, *J. Geophys. Res.*, *72*, 3595–3607.
- Johns, R. A., and P. V. Roberts (1991), A solute transport model for channelized flow in a fracture, *Water Resour. Res.*, *27*, 1797–1808.
- Keller, A. A., P. V. Roberts, and M. J. Blunt (1999), Effect of fracture aperture variations on the dispersion of contaminants, *Water Resour. Res.*, *35*, 55–64.
- Mandelbrot, B. (1982), *The Fractal Geometry of Nature*, 460 pp., W. H. Freeman, New York.
- McKenna, S. A., L. C. Meigs, and R. Haggerty (2001), Tracer tests in a fractured dolomite: 3. Double-porosity, multiple-rate mass transfer processes in convergent flow tracer tests, *Water Resour. Res.*, *37*, 1143–1154.
- Meerschaert, M. M., and C. Tadjeran (2003), Finite difference approximations for fractional advection-dispersion flow equations, *J. Comput. Appl. Math.*, *172*, 65–77.
- Meerschaert, M. M., D. A. Benson, P. Becker-Kern, and H.-P. Scheffler (2003), Governing equations and solutions of anomalous random walk limits, *Phys. Rev. E*, *66*, 060102(R).
- Miller, K., and B. Ross (1993), *An Introduction to the Fractional Calculus and Fractional Differential Equations*, John Wiley, Hoboken, N. J.
- Moench, A. F. (1989), Convergent radial dispersion: A Laplace transform solution for aquifer tracer testing, *Water Resour. Res.*, *25*, 439–447.
- Molz, F. J., G. J. Fix, and S. Lu (2002), A physical interpretation for the fractional derivative in Lévy diffusion, *Appl. Math. Lett.*, *15*, 907–911, doi:10.1016/S0893-9659(02)00062-9.
- Montroll, E. W., and G. H. Weiss (1965), Random walks on lattices, II, *J. Math. Phys.*, *6*, 167–181.
- Moreno, L., I. Neretnieks, and T. Eriksen (1985), Analysis of some laboratory tracers in natural fissures, *Water Resour. Res.*, *21*, 951–958.
- Moreno, L., Y. W. Tsang, C. F. Tsang, F. V. Hale, and I. Neretnieks (1988), Flow and tracer transport is a single fracture: A stochastic model and its relation to some field observations, *Water Resour. Res.*, *24*, 2033–2048.
- Moreno, L., C. F. Tsang, Y. Tsang, and I. Neretnieks (1990), Some anomalous features of flow and solute transport arising from fracture aperture variability, *Water Resour. Res.*, *26*, 2377–2391.
- Mourzenko, V. V., J.-F. Thovert, and P. M. Adler (1995), Permeability of a single fracture: Validity of the Reynolds equation, *J. Phys. II Fr.*, *5*, 465–482.
- Oldham, K. B., and J. Spanier (1974), *The Fractional Calculus*, Elsevier, New York.
- Paradisi, P., R. Cesari, F. Mainardi, and F. Tampieri (2001), The fractional Fick's law for non-local transport processes, *Physica A*, *293*, 130–142.
- Podlubny, I. (1999), *Fractional Differential Equations*, Elsevier, New York.
- Reimus, P. W. (2003), A refined approach to estimating effective flow porosity from cross-hole tracer tests in fractured media, paper presented at the 10th International High-Level Radioactive Waste Management Conference, Am. Nucl. Soc., Las Vegas, Nev., 30 March–2 April.
- Reimus, P. W., G. Pohll, T. Mihevc, J. Chapman, M. Haga, B. Lyles, S. Kosinski, R. Niswonger, and P. Sanders (2003), Testing and parameterizing a conceptual model for solute transport in a fractured granite using multiple tracers in a forced-gradient test, *Water Resour. Res.*, *39*(12), 1356, doi:10.1029/2002WR001597.
- Sabir, I. H., J. Torgersen, S. Haldorsen, and P. Aleström (1999), DNA tracers with information capacity and high detection sensitivity tested in groundwater studies, *Hydrogeol. J.*, *7*, 264–272, doi:10.1007/s100400050200.
- Saichev, A. I., and G. M. Zaslavsky (1997), Fractional kinetic equations: Solutions and applications, *Chaos*, *7*, 753–764.
- Samko, S., A. Kilbas, and O. Marichev (1993), *Fractional Integrals and Derivatives: Theory and Applications*, Gordon and Breach, New York.
- Scalas, E., R. Gorenflo, and F. Mainardi (2001), Uncoupled continuous-time random walks: Solution and limiting behavior of the master equation, *Phys. Rev. E*, *69*, 011107.

- Schumer, R. (2002), *Fractional Derivatives, Continuous Time Random Walks, and Anomalous Solute Transport*, Ph.D. thesis, Univ. of Nev., Reno.
- Schumer, R., D. A. Benson, M. M. Meerschaert, and S. W. Wheatcraft (2001), Eulerian derivation of the fractional advection-dispersion equation, *J. Contam. Hydrol.*, *38*, 69–88.
- Schumer, R., D. A. Benson, M. M. Meerschaert, and B. Baeumer (2003), Fractal mobile/immobile solute transport, *Water Resour. Res.*, *39*(10), 1296, doi:10.1029/2003WR002141.
- Shlesinger, M. F., J. Klafter, and Y. M. Wong (1982), Random walks with infinite spatial and temporal moments, *J. Stat. Phys.*, *27*, 499–512.
- Thompson, M. E. (1991), Numerical simulation of solute transport in rough fractures, *J. Geophys. Res.*, *96*, 4157–4166.
- Tsang, Y. W. (1995), Study of alternative tracer tests in characterizing transport in fractured rocks, *Geophys. Res. Lett.*, *22*, 1421–1424.
- Tsang, Y. W., and C. F. Tsang (1987), Channel model of flow through fractured media, *Water Resour. Res.*, *23*, 467–479.
-
- D. A. Benson and G. Pohl, Desert Research Institute, 2215 Raggio Parkway, Reno, NV 89512, USA. (dbenson@dri.edu; pohl@dri.edu)
- I. Farnham, Stoller Navarro Joint Venture, 7710 West Cheyenne, Las Vegas, NV 89129, USA. (irene.farnham@nv.doe.gov)
- M. M. Meerschaert, Department of Physics, Graduate Program of Hydrologic Sciences, University of Nevada, Reno, NV 89557, USA. (mcubed@unr.edu)
- C. Tadjeran, Department of Mathematics and Statistics, University of Nevada, Reno, NV 89557-0084, USA. (tadjeran@unr.edu)